J Mater Sci (2006) 41:8093–8100
DOI 10.1007/s10853-006-0646-y

The preparation of LPS SiC-fibre-reinforced SiC ceramics using electrophoretic deposition

S. Novak · K. Mejak · G. Dražić

Received: 12 January 2006 / Accepted: 6 July 2006 / Published online: 28 October 2006

Abstract With the aim of determining the possibility of producing SiC-based ceramic-matrix composites using the electrophoretic deposition (EPD) technique, the effect of the composition of SiC-based suspensions on the deposition was studied. Ethanol suspensions of two different grades of SiC powders, with and without the addition of a sintering aid, were used for depositing on steel electrodes or on SiC-fibres. The pH of the suspensions, the solids loading and the particle size were shown to have a strong influence on the deposition process and on the properties of the fresh deposits. The overall results demonstrate that by using appropriate conditions for the EPD, a firm SiC-based deposit can be collected at the SiC-fibres and after suitable thermal treatment, a pore-free SiC-matrix, well adhered to the SiC fibres, can be achieved.

Introduction

Continuous-fibre-reinforced ceramics are a group of materials with significantly better mechanical properties than monolithic or particulate composites. In the past decade various composites with fibres were developed in which continuous fibres of carbon, alumina or silicon carbide were used to provide the reinforcement for various ceramic matrixes [1, 2]. The main role of the fibres is to cause the deflection of any initiated crack and hence to dissipate its energy in order to protect the material from catastrophic fracture. Due to their outstanding high-temperature behaviour, SiC-fibre-reinforced SiC ceramics are used in various applications that are subject to extreme conditions, for example, in aerospace. Lately, SiC_f/SiC composites have also been considered to be one of the best candidates for use in future fusion reactors, where, in addition to the high-temperature mechanical and physical properties of the SiC, a low neutron activation is one of the critical requirements for the material [3, 4]. At present, the main limitation when it comes to producing a material to meet the requirements of this highly demanding application is a lack of suitable manufacturing technique. Various methods of SiC-fibre-preform infiltration have been considered, such as chemical vapour infiltration (CVI), polymer infiltration and pyrolysis (PIP), nanopowder infiltration and transient eutectoid (NITE) as well as the simple immersion of ceramic slurries and combinations of these methods [5–10]. From among these methods the most attractive for producing a material for fusion applications appears to be CVI; however, this is an extremely slow and costly process and seems to be unable to produce material without open pores, and consequently one of the important requirements—gas impermeability—is difficult to achieve. In other processes, the high temperatures needed to produce sufficient density and a large shrinkage of the material present serious drawbacks.

In our investigations we looked at the potential of electrophoretic deposition (EPD) as a possible technique for the infiltration of a SiC-fibre preform to produce a SiC_f/SiC composite, providing that a suitable

S. Novak (✉) · K. Mejak · G. Dražić
Department of Nanostructured Materials, Jozef Stefan Institute, Jamova 39, Ljubljana SI-1000, Slovenia
e-mail: sasa.novak@ijs.si

additive for densification is used. Various reports show that EPD has been successful for preparing thick and thin films and various free-standing materials [11–13], for example, bulk SiC-based ceramics with boron, carbon, Al_2O_3 or AlN as sintering additives [14–16]. Another example of using EPD is the infiltration of alumina or carbon fibres woven with a ceramic matrix [17, 18]. For the material to be used in the first wall of a fusion reactor, suitable low-neutron-activation sintering additives must be used. Such additives would allow low-temperature densification without any detrimental effects on the fibres. This excludes the conventional additives for SiC, such as B, C, and additives from the system Al_2O_3(AlN)-Y_2O_3 that require high sintering temperatures, typically above 1800 °C. In our study two grades of the SiC powder was used and a phosphate glass was employed as the additive; this enables densification below the temperature limit of 1500 °C at close-to-zero shrinkage. The conditions for the EPD of a SiC-based matrix material on SiC-fibres were investigated.

Experimental

Two grades of SiC powder were used in this investigation: ''μ-SiC'', a submicron β-SiC BF-12 (H. Starck, Goslar, Germany) with an average particle size of 0.5 μm; and ''nano-SiC'', a powder with an average particle size of 50 nm (Hefei Kiln Nanom.Technol. Dev. Co. Ltd, China). Aluminium phosphate, ''AP'', (TKI doo, Slovenia) was used as an additive for the densification. The suspensions of the powder and the additive in ethanol were prepared by homogenisation in a ball-mill for at least 2 h. The characteristics of the particles in the suspensions were quantified by measuring the zeta-potential (ZP) using a ZetaPals zetameter (Brookhaven, USA). The operational pH was adjusted using HCl, citric acid or NH_4OH, and measured with a pH meter (Metron Ltd, Switzerland). For simplicity, the measured values are designated as ''pH'' in this investigation. Surface chemistry of the powders was analysed by X-ray photoelectron spectroscopy (XPS) using TFA spectrometer (Pysical Electronics, USA).

The EPD experiments were performed at a constant voltage of 60 V. The electrodes were either square stainless steel plates, 2×2 cm^2, placed vertically at a distance of 2 cm, or a bundle of the SiC fibres (Nicalon, Nippon Carbon Co., Ltd). The solids content in the suspensions for the EPD varied from 15 wt.% (4.3 vol.%) to 70 wt.% (37.3 vol.%). During the deposition the electrical current and the weight change of the deposit were monitored continuously. The densities of the fresh (wet) deposits were calculated from the buoyancy in the suspension, and the solids content in the deposits was determined by measuring the weight change during drying. The deposits were fired at temperatures from 1300 to 1500 °C in an Ar atmosphere. The sintered samples were inspected by SEM, TEM and EDS.

Results and discussion

Figure 1 shows the zeta-potential for the used powders in an ethanol suspension as a function of pH. It is clear that the point of zero charge (PZC) for the μm-SiC powder appears at about pH 6.0. At lower values the particles carry a relatively high positive net-charge, while the ZP in the alkaline region are negative. The addition of aluminium phosphate (AP) shifted the PZC to a lower value, suggesting that it is adsorbed on the surface of the SiC particles. The measured ZP values for the nano-SiC powder were much lower than those for the μm-SiC across the whole range of pH. The PZC appears at a lower pH value, suggesting that the fine SiC particles have an oxidised surface layer. Figures 2a and b show the morphology of the μm-SiC and nano-SiC powders, while Figs. 2c and d show HRTEM images of the oxygen-containing amorphous surface layers on the particles of both powders. In Figs. 2e and f EDXS spectra of the amorphous layer and bulk SiC particle of μm-SiC are shown. It is demonstrated, that the thickness of the layers is similar for both powders (1–2 nm). The XPS analysis revealed presence of oxycarbides at the surface of the μm-SiC powder, while in the nano-SiC powder, beside oxycarbides also SiO_2 was found.

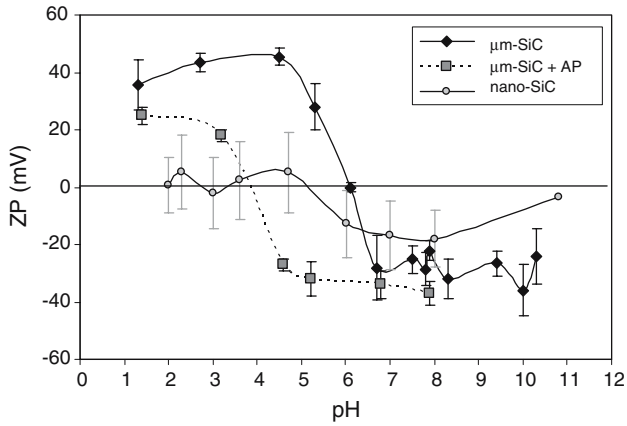

Fig. 1 Zeta-potential of μm-SiC (without and with addition of aluminium phosphate) and nano-SiC powders in ethanol as a function of pH

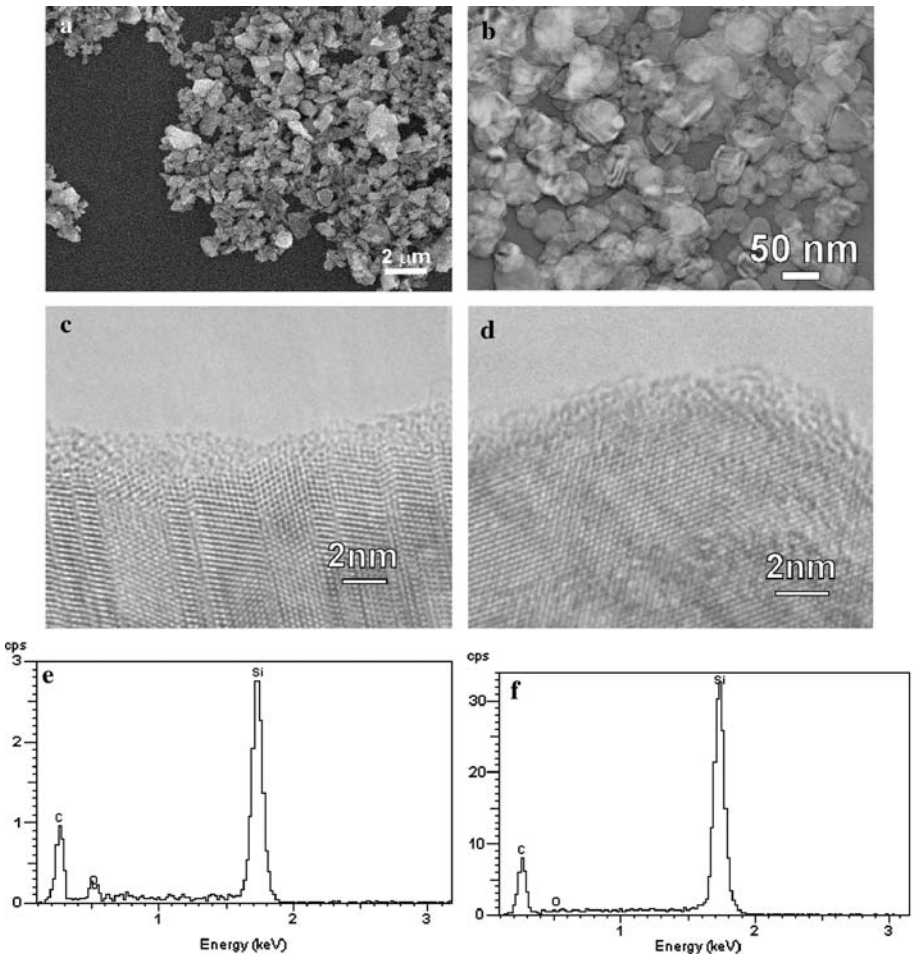

Fig. 2 (**a**) - SEM micrograph of μm-SiC, (**b**) - TEM micrograph of nano-SiC powder, (**c**), (**d**) - HRTEM micrographs of the amorphous layer on SiC particle in μm-SiC and nano-SiC powders; (**e**), (**f**) - EDX spectra of the surface layer and bulk particle in μm -SiC sample

In order to better understand the process, suspensions of μm-SiC powder were deposited without any sintering additive on steel electrodes. The pH values were selected in accordance with the characteristic points in the ZP vs. pH graph in Fig. 1: the natural pH of the suspension (pH 5.0) and the pH values where the ZP appears highly positive or negative (pH 2.8 and 11, respectively). The solids content in the starting suspension was 50 wt.% and the density was 1.26 g/cm^3. In another set of experiments, the solids content in the suspensions was varied from 30 to 70 wt.%, keeping the pH value constant. The solids content in the as-formed (wet) deposits, the deposition rate and the current change during the depositions are presented in Figs. 3a–f.

The EPD of the suspension with the natural pH (i.e., pH 5.0) resulted in a very loose deposit being formed at the cathode. After approximately 10 min, when its weight exceeded approximately 10 g, it slipped from the electrode. Obviously, under the given conditions, the initially low-viscosity suspension flocculated at the electrode and hence its viscosity increased. The fresh deposit (i.e., before drying) was found to contain only 59.1 wt.% (26.8 vol.%) solids (Fig. 3a). Due to the low solids content, such a visco-elastic deposit is not able to resist its own weight: when the force of gravity overcomes the weak interparticle forces, the viscous-flow behaviour predominates over the elastic behaviour and the deposit returns to the state of a viscous liquid.

As expected, at pH values close to the PZC no deposit was formed. At pH 11 the deposit formed at the anode in accordance with the ZP vs. pH relationship presented in Fig. 1. It contained 67.8 wt.% (34.9 vol.%) of solids (Fig. 3a), which is higher than that obtained from the suspension at natural pH. The rate of deposition was also higher than at pH 2.8 and pH 5 (Fig. 3c); this could be related to the larger amount of electrolyte needed for the pH adjustment, which is also reflected in the higher initial current (Fig. 3e). Resulting lower solids content and a lower density of the deposit formed at pH 11 can be explained by the lower ZP than at pH 2.8.

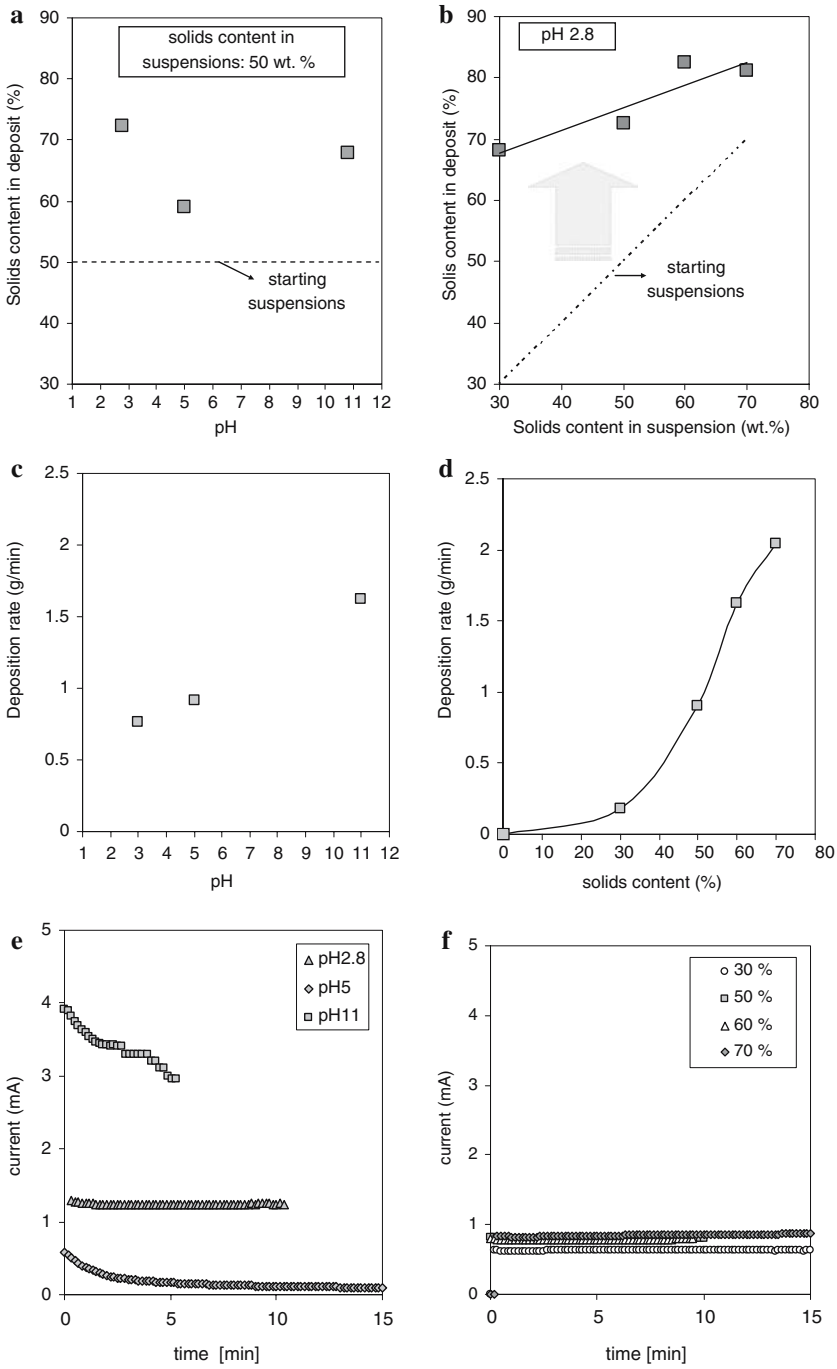

Fig. 3 Solids content in fresh deposit of μm-SiC as a function of (**a**) - pH and (**b**) - solids content in starting suspensions; deposition rate as a function of (**c**) - pH and (**d**) - solids content in the suspensions; electrical current change during the deposition as a function of (**e**)- pH and (**f**) - solids content (60 V, steel electrode; suspension in (**a**), (**c**), (**e**): 50 wt. % solids; suspensions in (**b**), (**d**), (**e**): pH 2.8)

From Fig. 3c it is obvious that the rate of deposition from the suspension with pH 2.8 was slightly lower than that at the natural pH 5. The deposit formed at the cathode and appeared to be much firmer in comparison to the deposit formed at the natural pH. Its density was 1.78 g/cm^3, which is significantly higher than the starting suspension, i.e., 1.26 g/cm^3. The solids content in the deposit was determined to be 72.3 wt.%, i.e., 40.1 vol.% (Fig. 3a).

In the next set of experiments, the effect of the solids content in the starting suspension was verified for the deposition of suspensions with 30–70 wt.% of the μm-SiC powder at a constant pH value of 2.8. Figures 3b and d reveal that the density of the deposits as well as the deposition rate increased with an increase in the powder content in the starting suspension. On the other hand, the effect of the solids content on the initial current in the suspensions, reflecting their

conductivity, was negligible (Fig. 3f). This suggests a minor contribution of the charged μm-SiC particles to the overall conductivity. Furthermore, no current drop during the deposition was observed.

The above results reveal that the consistency of the deposit, evaluated in this study on the basis of its density and the solids content, is governed primarily by the surface charge on the particles. The deposits with the highest density were obtained by depositing from the acidic suspension in which the SiC particles carried the highest charge, while the current was kept at a limited value by keeping the concentration of ions low (small electrolyte additions). The density as well as the deposition rate increased with the solids content in the starting suspensions. It should also be pointed out that a minor current drop during the EPD was observed when a deposit with high solids content (72.3 wt.%) was formed, i.e. at pH 2.8. In contrast, a significant current drop was observed at pH 5 and 11 where deposits with lower densities were formed. This is not in agreement with the assumption that the current drop is caused by the inhibited transport of charge carriers due to the accumulation of the deposit at the electrode. Further, according to the results presented in Figs. 3e and f, the major charge carrier in the analysed suspensions was the ions, while the charged particles make a minor contribution. Hence, it is reasonable to assume that a large particle separation in the deposits containing up to 81 wt.% solids, i.e. 52 vol.% (see Fig. 3b, f) allows the ions, as the proposed major charge carriers, to move towards the electrode through the deposit.

Additional EPD experiments were performed with the nano-SiC powder. Due to a high apparent viscosity of the suspensions, resulting from a high specific surface area of the powder, a suspension with a maximum of 17 wt.% was used for the EPD. As a result, in accordance with the above-presented dependence of deposition rate on the solids content in the suspensions, the deposition rate was only 0.25 g/min. The deposit was very loose, and after 10 min of deposition it slipped from the electrode. As presented in Fig. 4, the initial current was much higher than that observed for all the analysed μm-SiC suspensions. This could be explained by the presence of surface silanol groups losing the proton in water containing solutions that reflects also in the natural acidity of the suspension (pH < 2). Furthermore, in contrast to the μm-SiC powder, where a negligible effect of the particles concentration on the conductivity was observed (see Fig. 3f), the dilution of the suspension caused a decrease in the initial current, suggesting that the small and numerous nano-SiC particles might also

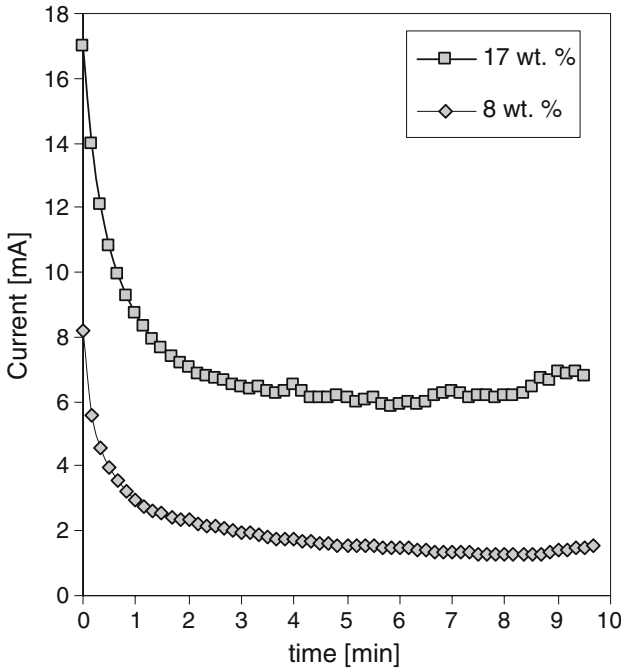

Fig. 4 Electrical current during the deposition of nano-SiC suspension as a function of solids content in the starting suspensions (60 V, steel electrode)

contribute to the conductivity of the suspensions. However, a lower concentration of silanol ions in the diluted suspensions might also have the same effect. Furthermore, during the deposition a significant current drop was also observed.

The addition of the AP changed not only the ZP vs. pH relationship, but also the course of the deposition. At the natural pH of the μm-SiC suspension with the AP addition, i.e. pH 2, the particles carry a low positive net charge, as presented in Fig. 1, and therefore they collect at the cathode. Figure 5 shows that the addition of the AP significantly increased the initial current, most probably due to a high concentration of free phosphate ions in the suspensions. The deposition rate was 0.3 g/min, which was much lower than for the suspension with a similar pH but without the additive (see Fig. 3c). As presented in Fig. 5, increasing the pH to 10, where the ZP was observed to have high negative value, resulted in a decreased initial current and an increase in the deposition rate to 0.8 g/min. The decreased conductivity suggests a decreased concentration of free ions due to a chemical reaction of phosphate ions with the added ammonium hydroxide.

In contrast, the deposition from the suspension of nano-SiC powder with the AP additive was only successful in acidic suspensions. However, even in this case the deposition was slow, and the deposits contained bubbles. The initial current was very high,

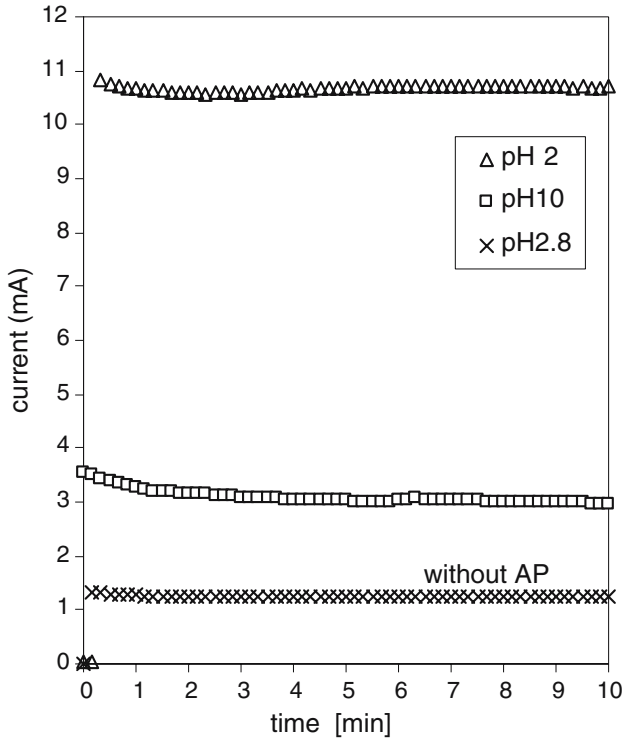

Fig. 5 The current during the deposition of μm-SiC suspension with the addition of aluminium phosphate as a function of solids content in the starting suspensions (60 V, steel electrode)

70 mA, and a significant current drop was observed during the deposition (Fig. 6a). This could be explained by the reduced active surface of the electrode due to the presence of bubbles. As shown in Fig. 6b, the bubbles were concentrated by the electrode, while the bulk deposit appears rather dense. Dilution of the suspension with ethanol diminished the current, as was also observed for the nano-SiC suspension without the AP addition.

As the main aim of the present study was the EPD of SiC with the AP addition on SiC-fibres, in further experiments a bundle of SiC-fibres was placed in the cell as the deposition electrode. Due to its small effective surface area, the initial current was only 3 mA. The pH of the suspension of nano-SiC powder with the addition of AP was 2.8 and the solids content was 35 wt.%. Figure 7 presents the current change during the deposition and the image of the bundle with the deposit. Due to the small quantity of the deposit on the fibres, the weight was not monitored. A visual inspection revealed an apparently relatively firm deposit on the SiC-bundle.

The SiC bundle with the deposit, composed of nano-SiC powder and AP, was sintered in an inert atmosphere at 1450 °C. The cross-section of the sintered sample was polished and inspected by SEM, TEM and EDS. The microstructures of the matrix were rather dense with a small amount of closed porosity, and good cohesion between the matrix and the fibres is evident (Figs. 8a and b). Due to a low firing temperature, the SiC-particle size remained practically unchanged, i.e., 50 nm (Fig. 8c). The EDS spectrum reveals a certain amount of oxygen in the matrix material, probably resulting primarily from the oxygen-containing layer on the nano-SiC particles.

Conclusions

In the present investigation the effect of the composition of SiC-based suspensions on EPD was studied with the aim of establishing the conditions for deposition on SiC-fibres. Ethanol suspensions of two different grades of SiC powders, with and without the addition of AP (as a sintering aid), were used for depositing on steel electrodes.

Fig. 6 (**a**) - The current change during the deposition of the suspension of nano-SiC powder and aluminium-phosphate as a function of solids content; (**b**) - image of the inner side of the deposit with bubbles

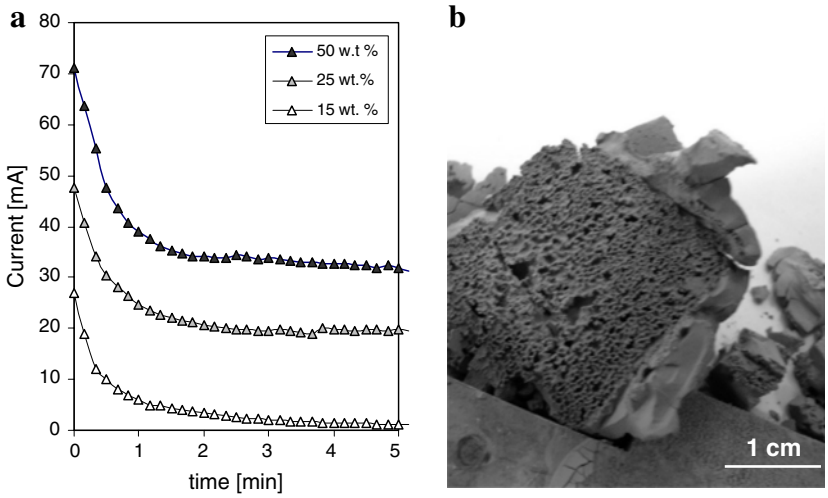

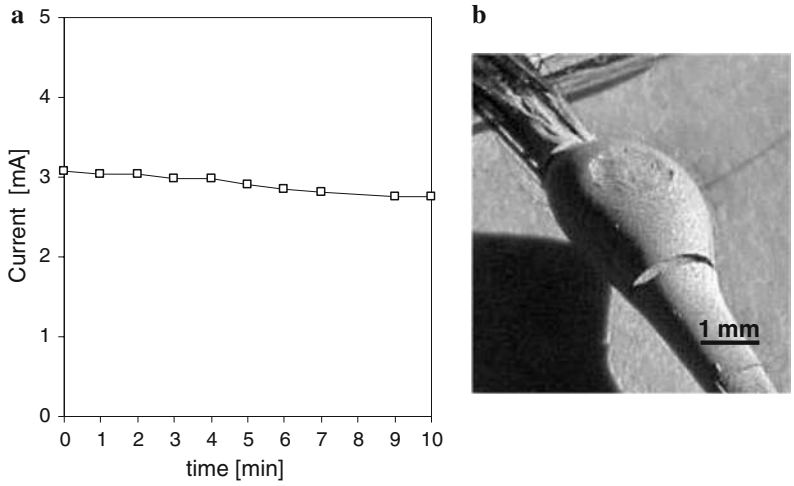

Fig. 7 (**a**) - The current change during the deposition of a suspension of nano-SiC powder with the addition of aluminum phosphate on a bundle of SiC-fibres (solids content: 10 wt. %); (**b**) - an image of the bundle with deposit

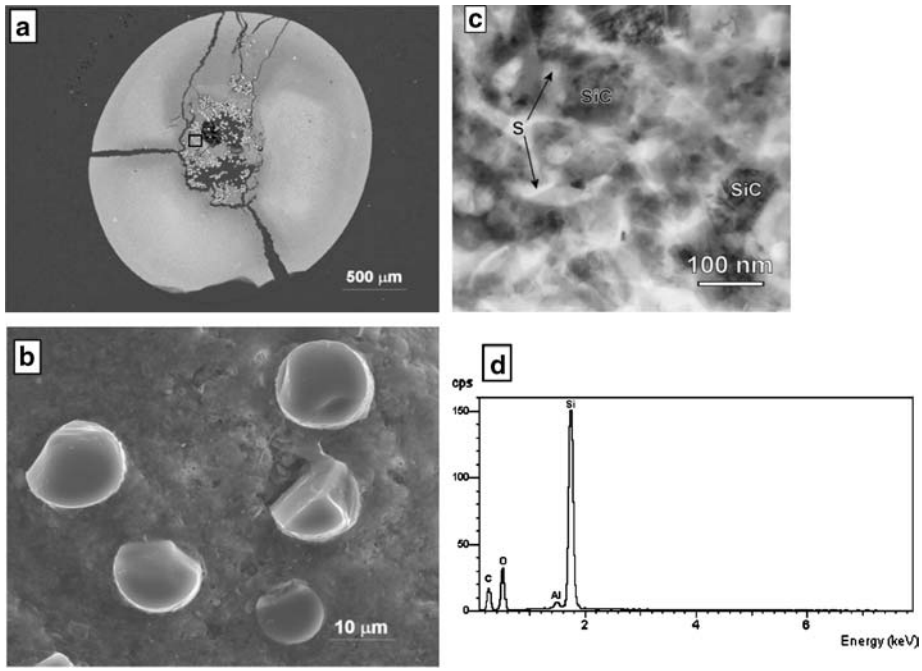

Fig. 8 (**a**), (**b**) - SEM micrographs of the sintered material with SiC-fibres; (**c**) and (**d**) TEM micrograph and EDS spectrum of the SiC-matrix, respectively

The results showed that the conductivity of the suspensions is strongly dependent on the amount of free ions. In the case of submicron SiC powder, the major charge carriers were ions, while the contribution of the nano-sized SiC powder is probably not negligible. The solids content in the fresh as-formed deposit increased with the surface charge on the particles. The solids content was also observed to have a beneficial effect in the analysed range, i.e., up to 70 wt.%. During the depositions, a current drop was normally observed for porous deposits containing bubbles. This suggests that the current drop was not caused by the inhibited transport of the charge carriers due to the accumulation of the deposit, but rather by the reduced active surface of the electrode.

The deposits with the highest packing density were obtained from highly loaded acidic suspensions of submicron SiC powder. The EPD of the nano-SiC powder was much less effective than that for the submicron SiC. This is presumably connected to the oxide layer on the particles, however, a full explanation will require further detailed studies. Aluminium phosphate, added as a sintering aid for SiC, as well as the use of nano-SiC powder, significantly changed the behaviour of the suspension. The large current at the used potential of 60 V and the formation of bubbles on the steel electrode were observed. In contrast, when the suspension with the nano-SiC powder and the sintering additive was deposited on the bundle of SiC fibres, the current

was low and no bubbles were observed in the deposit.

Acknowledgement The work was financially supported by the European Commission Euratom/Fusion and by the Ministry of High Education, Science and Technology of Republic of Slovenia. The XPS analysis of the powders were performed by Dr. J. Kovac.

References

1. Krenkel W (2005) In: Bansal NP (ed) Handbook of ceramic composites. Kluwer, Boston, p 117
2. Keller KA, Jefferson G, Kerans R (2005) In: Bansal NP (ed) Handbook of ceramic composites. Kluwer, Boston, p 377
3. Tavassoli AAF (2002) J Nucl Mater 302:73
4. Jones RH, Giancarli L, Hasegawa A, Katoh Y, Kohyama A, Riccardi B, Snead LL, Weber WJ (2002) J Nucl Mater 307:1057
5. Naslain R (2004) Comp Sci Technol 64(2):155
6. Igawa N, Taguchi T, Nozawa T et al (2005) J Phys Chem Solids 66:551
7. Nannetti CA, Riccardi B, Ortona A, La Barbera A, Scafe E, Vekinis G (2002) J Nucl Mater 307–311:1196
8. Katoh Y, Kohyama A, Nozawa T et al (2004) J Nucl Mater 329:587
9. Nannetti CA, Ortona A, de Pinto DA et al (2004) J Am Ceram Soc 87:1205
10. Novak S, Drazic G (2005) Slip-infiltration of SiC-fiber preforms for production of sicf/sic composites, 12th Int. conf. on fusion reactor materials, Santa Barbara, CA, USA
11. Boccaccini AR, Zhitomirsky I (2002) Curr Opin Solid State Mater Sci 6:251
12. Van der Biest O, Put S, Anne G, Vleugels J (2004) J Mater Sci 39:779
13. Fukada Y, Nagarajan N, Mekky W, Bao Y, Kim HS, Nicholson PS (2004) J Mater Sci 39:787
14. Vandeperre L, Van der Biest O, Bouyer F, Persello J, Foissy A (1997) J Eur Ceram Soc 17:373
15. Bouyer F, Foissy A (1999) J Am Ceram Soc 82(8):001
16. Moritz K, Muller E (2002) Key Eng Mat 206(2):193
17. Boccaccini AR, Kaya C, Chawla KK (2001) Composites A – Appl Sci Manuf 32(8):997
18. Boccaccini AR (2004) Mater Sci Forum 221